

Measurement of the Solar Neutrino Capture Rate by the Russian-American Gallium Solar Neutrino Experiment During One Half of the 22-Year Cycle of Solar Activity

J. N. Abdurashitov, V. N. Gavrin, S. V. Girin, V. V. Gorbachev, P. P. Gurkina,
T. V. Ibragimova, A. V. Kalikhov, N. G. Khairnasov, T. V. Knodel, I. N. Mirmov,
A. A. Shikhin, E. P. Veretenkin, V. M. Vermul, V. E. Yants, and G. T. Zatsepin
Institute for Nuclear Research, Russian Academy of Sciences, 117312 Moscow, Russia

T. J. Bowles and W. A. Teasdale
Los Alamos National Laboratory, Los Alamos, New Mexico 87545, USA

J. S. Nico
National Institute of Standards and Technology, Stop 8461, Gaithersburg, Maryland 20899, USA

B. T. Cleveland, S. R. Elliott, and J. F. Wilkerson
University of Washington, Seattle, Washington 98195, USA

(The SAGE Collaboration)
(Dated: 2 December 2024)

We present the results of measurements of the solar neutrino capture rate in gallium metal by the Russian-American Gallium Experiment SAGE during slightly more than half of a 22-year cycle of solar activity. Combined analysis of the data of 92 runs during the 12-year period January 1990 through December 2001 gives a capture rate of solar neutrinos with energy more than 233 keV of $70.8^{+5.3}_{-5.2}$ (stat.) $^{+3.7}_{-3.2}$ (syst.) SNU. This represents only slightly more than half of the predicted standard solar model rate of 130 SNU. We give the results of new runs beginning in April 1998 and the results of combined analysis of all runs since 1990 during yearly, monthly, and bimonthly periods. Using a simple analysis of the SAGE results combined with those from all other solar neutrino experiments, we estimate the electron neutrino pp flux that reaches the Earth to be $(4.6 \pm 1.1) \times 10^{10} / (\text{cm}^2 \cdot \text{s})$. Assuming that neutrinos oscillate to active flavors the pp neutrino flux emitted in the solar fusion reaction is approximately $(7.7 \pm 1.8) \times 10^{10} / (\text{cm}^2 \cdot \text{s})$, in agreement with the standard solar model calculation of $(5.95 \pm 0.06) \times 10^{10} / (\text{cm}^2 \cdot \text{s})$.

PACS numbers: 26.65.+t, 96.60.-j, 95.85.Ry, 13.15.+g

I. INTRODUCTION

There has been outstanding progress in solar neutrino research in the last several years. The large water Cherenkov detectors SuperKamiokande (SK) [1] and the Sudbury Neutrino Observatory (SNO) [2] have begun to measure the high-energy solar neutrinos from ^8B decay in real time with a high counting rate. The results from these two neutrino telescopes of a new generation add significant information to the existing results from the chlorine [3] and gallium [4, 5] radiochemical experiments and the Kamiokande experiment [6]. The elastic scattering results of SK combined with the charged current results from SNO indicate that, in addition to electron neutrinos, active neutrinos of other flavors are reaching the Earth from the Sun. The combined analysis of results of all these experiments gives convincing evidence that part of the electron neutrinos formed in thermonuclear reactions in the Sun change their flavor on their way to the Earth.

Further measurement of the details of flavor conversion for solar neutrinos requires a new generation of neutrino

telescopes that will be sensitive to the spectrum below 2 MeV, a region that contains the proton-proton (pp) and CNO continua as well as the ^7Be and pep lines. Although there are many promising ideas for real-time low-energy neutrino detectors [7], at the present time only the radiochemical gallium experiments are able to measure and monitor this part of the solar neutrino spectrum. The 233-keV threshold of the reaction $^{71}\text{Ga}(\nu_e, e^-)^{71}\text{Ge}$ [8] enables one to measure the pp neutrinos, the principal component of the solar neutrino spectrum. If we exclude exotic hypotheses, the rate of the pp reaction is directly related to the solar luminosity and is insensitive to alterations in the solar models that influence the subsequent reactions in the solar fusion chain.

The neutrino capture rate in ^{71}Ga predicted by the Standard Solar Model (SSM) [9] is 130^{+9}_{-7} SNU, with the main contribution of 69.7 SNU from the pp neutrinos ¹. Contributions by ^7Be and ^8B neutrinos are 34.2 SNU

¹ 1 SNU = 1 interaction/s in a target that contains 10^{36} atoms of the neutrino absorbing isotope.

and 14.2 SNU, respectively. The insensitivity of Ga to variation in the solar model is seen in the independently calculated result of 127.2 SNU [10] for the total capture rate.

From the results of the SNO and SK experiments we now have a high accuracy measurement of the ${}^8\text{B}$ flux that reaches the Earth and its electron neutrino component. In the near future it is expected that the KamLAND experiment [11] will greatly restrict the range of possible electron neutrino mixing parameters. This data, combined with results from the Borexino experiment [12], will give us a good measurement of the ${}^7\text{Be}$ flux from the Sun. By subtracting the ${}^7\text{Be}$ and ${}^8\text{B}$ components from the total signal in the Ga experiment, we will obtain a measurement of a fundamental astrophysical parameter — the neutrino flux from the proton-proton fusion reaction. There will be a slight contamination from the CNO and *pep* neutrinos but this can be removed with the information from the Cl experiment. A rough estimate of the *pp* neutrino flux using the information that we have now is presented in the next to last section. Since in the immediate future only the Ga experiments provide this measurement, it is very important that both SAGE [4] and GALLEX's successor GNO [13] continue to operate so as to improve the accuracy of their results.

The experimental layout and procedures, including extraction of germanium from gallium, counting of ${}^{71}\text{Ge}$, and data analysis, are described in detail in our article “Measurement of the solar neutrino capture rate with gallium metal” in Physical Review C [4]. That article gives the SAGE results for the period January 1990 through December 1997. Since it contains a complete description of the experiment and the analysis techniques, we refer the reader who wishes further detail to that publication. Here we briefly discuss the main principles of the experiment, give the statistical analysis of the data from 1998–2001, present new results for some systematic uncertainties, and conclude with the current implications of the SAGE result for solar and neutrino physics.

II. OVERVIEW OF THE SAGE EXPERIMENT

A. The Laboratory of the Gallium Germanium Neutrino Telescope

The SAGE experiment is situated in a specially built deep underground laboratory [14] at the Baksan Neutrino Observatory (BNO) of the Institute for Nuclear Research of the Russian Academy of Sciences in the northern Caucasus mountains. It is located 3.5 km from the entrance of a horizontal adit excavated into the side of Mount Andyrchi. The main chamber of the laboratory is 60 m long, 10 m wide, and 12 m high. The rock gives an overhead shielding equivalent to 4700 m of water and reduces the muon flux by a factor of 10^7 . The measured muon flux is $(3.03 \pm 0.10) \times 10^{-9}/(\text{cm}^2\text{-s})$ [15]. To reduce neutron and gamma backgrounds from the rock, the laboratory

is entirely lined with 60 cm of low-radioactivity concrete with an outer 6 mm steel shell. The flux of neutrons with energy (1–11) MeV is less than $2.3 \times 10^{-7}/(\text{cm}^2\text{-s})$ [16]. All facilities required by the experiment are in this underground area, with additional rooms devoted to chemistry, counting, and a low-background solid-state Ge detector. Subsidiary measurements are made in a general laboratory building outside the adit.

B. Experimental Procedures

The gallium target used at the present time for measurements is about 50 t. It is in the form of liquid metal and is contained in 7 chemical reactors. A measurement of the solar neutrino capture rate, which we call a “run”, begins by adding to the gallium a stable Ge carrier. The carrier is a Ga-Ge alloy with a known Ge content of approximately 350 μg and is distributed equally among all reactors. The reactor contents are stirred thoroughly to disperse the Ge throughout the Ga mass. After a typical exposure interval of 4 weeks, the Ge carrier and ${}^{71}\text{Ge}$ atoms produced by solar neutrinos and background sources are chemically extracted from the Ga using procedures described elsewhere [4, 17]. The final step of the chemical procedure is the synthesis of germane (GeH_4), which is used as the proportional counter fill gas with an admixture of (80–90)% Xe. The total efficiency of extraction is the ratio of mass of Ge in the germane to the mass of initial Ge carrier and is typically in the range of (80–90)%. The systematic uncertainty in this efficiency is 3.4%, mainly arising from uncertainties in the mass of added and extracted carrier. Each extraction dissolves $\sim 0.1\%$ of the gallium. Ga metal is regenerated from the accumulated extracted solutions, purified, and subsequently will be returned to the target.

The proportional counter is placed in the well of a NaI detector that is within a large passive shield and is counted for a typical period of 4–6 months. ${}^{71}\text{Ge}$ decays via electron capture to ${}^{71}\text{Ga}$ with a half-life of 11.43 d. Low energy *K*- and *L*-shell Auger electrons and x rays from electron shell relaxation produce a nearly point-like ionization in the counter gas, resulting in a fast rise time for the pulse from the counter. In contrast, most background events leave an extended trail of ionization, producing a slower rise time. A candidate ${}^{71}\text{Ge}$ event must thus have an energy within a window around an *L* or *K* peak and must also have a rise time consistent with point-like ionization. In addition, since ${}^{71}\text{Ge}$ decays without gamma emission, this event must not be coincident with an event in the NaI detector.

The data acquisition electronics have evolved over the course of SAGE. During the first two years a hardware measure of the pulse rise time was used — the amplitude of the differentiated pulse (ADP) technique. This method suffices well in the *K* peak (10.4 keV) but was found to be inadequate for the *L* peak (1.2 keV), which is more sensitive to electronic drifts and has higher back-

TABLE I: Parameters for all runs beginning with April 1998 that are used to give the solar neutrino result. The efficiency values include the reduction for the energy cut (0.9815), for the rise time cut (0.95), and for the faulty data acquisition program for runs prior to 2000 (0.76). The ‘Peak ratio’ is the factor by which an ^{55}Fe calibration must be multiplied to correct the energy scale; it is 1.0 for a counter with no polymerization.

Mean Exposure date	Exposure date	Exposure time (days)	Ga mass (t)	Extraction efficiency	Counter name	Pressure (mm Hg)	Percent GeH ₄	Operating voltage	K-peak efficiency	L-peak efficiency	Peak ratio
Apr. 98	1998.225	44.9	48.05	0.85	A13	695	37.0	1480	0.243	0.219	1.01
May 98	1998.347	30.0	51.17	0.91	LY4	690	29.5	1366	0.238	0.245	1.00
July 98	1998.477	45.6	51.06	0.90	A12	680	32.0	1414	0.235	0.237	1.00
Aug. 98	1998.611	45.7	50.93	0.89	LA51	660	27.0	1356	0.234	0.244	1.04
Oct. 98	1998.745	45.8	50.81	0.92	A13	680	32.0	1404	0.244	0.212	1.00
Nov. 98	1998.883	45.8	50.68	0.92	LY4	680	26.5	1322	0.238	0.244	1.00
Jan. 99	1999.014	44.7	50.54	0.92	A12	700	30.0	1398	0.239	0.241	1.00
Feb. 99	1999.130	38.7	50.43	0.89	LA51	705	11.0	1194	0.248	0.234	1.05
Apr. 99	1999.279	51.7	50.29	0.89	A13	665	13.5	1206	0.253	0.231	1.05
June 99	1999.417	46.7	50.17	0.87	LY4	670	11.0	1140	0.246	0.239	1.00
July 99	1999.551	45.7	50.06	0.90	LA116	635	12.5	1164	0.243	0.244	1.03
Sep. 99	1999.685	45.7	49.91	0.91	LA51	660	11.5	1172	0.242	0.238	1.05
Oct. 99	1999.801	38.7	49.78	0.90	A13	665	12.5	1186	0.254	0.202	1.01
Jan. 00	2000.035	28.8	49.59	0.91	LA51	700	13.5	1224	0.324	0.310	1.05
Feb. 00	2000.127	30.7	49.48	0.83	LY4	646	10.4	1130	0.320	0.316	1.01
Mar. 00	2000.207	28.8	49.42	0.91	A13	665	14.5	1206	0.332	0.329	1.10
May 00	2000.359	30.7	49.24	0.92	LA116	705	14.0	1244	0.329	0.315	1.03
June 00	2000.451	33.7	49.18	0.84	LA51	652	12.0	1160	0.317	0.314	1.03
July 00	2000.540	32.0	49.12	0.92	LY4	670	13.8	1182	0.321	0.316	1.01
Aug. 00	2000.626	31.3	49.06	0.73	A13	707	9.5	1176	0.343	0.321	1.08
Sep. 00	2000.704	27.7	49.00	0.89	A12	690	14.7	1224	0.324	0.312	1.00
Oct. 00	2000.796	30.7	48.90	0.84	LA116	734	9.4	1188	0.337	0.303	1.03
Nov. 00	2000.876	28.7	48.84	0.93	LA51	680	11.9	1196	0.345	0.330	1.03
Dec. 00	2000.958	30.7	48.78	0.93	LY4	697	12.0	1174	0.327	0.312	1.02
Feb. 01	2001.122	29.8	41.11	0.87	LA116	687	9.2	1144	0.330	0.314	1.04
Mar. 01	2001.214	33.4	48.53	0.92	LA51	635	13.5	1180	0.314	0.317	1.02
Apr. 01	2001.290	22.7	48.43	0.90	YCT1	695	13.1	1210	0.344	0.333	1.00
May 01	2001.373	31.7	48.37	0.88	YCT2	625	14.9	1178	0.332	0.342	1.00
June 01	2001.469	31.7	48.27	0.92	YCT3	678	12.2	1190	0.342	0.334	1.00
July 01	2001.547	23.7	48.17	0.93	LA116	690	12.7	1196	0.328	0.315	1.03
Aug. 01	2001.624	28.7	48.11	0.59	A12	768	7.2	1148	0.340	0.302	1.00
Sep. 01	2001.701	27.7	48.06	0.90	YCT1	665	15.0	1204	0.338	0.337	1.00
Oct. 01	2001.793	30.7	47.96	0.88	YCT2	758	12.2	1210	0.354	0.326	1.00
Nov. 01	2001.887	34.8	47.91	0.92	YCT3	685	14.2	1210	0.342	0.335	1.00
Dec. 01	2001.955	22.8	47.86	0.86	YCT4	685	11.4	1176	0.344	0.333	1.00

ground. In 1992 an 8-channel counting system with a 1-GHz digital oscilloscope was implemented, which permits off-line analysis of the event waveforms. The digitized pulse is fit to a functional form [18] which gives the energy deposited during the event and the time duration T_N over which the ionization arrives at the anode wire. All L -peak results and the vast majority of K -peak results are obtained from this waveform analysis.

After filling, counters are calibrated with an ^{55}Fe source (5.9 keV) through a window in the Fe cathode. Typically, they are again calibrated after 3 days of operation and approximately every two weeks subsequently. Calibrations are also made with a ^{109}Cd source whose gamma rays penetrate the counter wall and fluoresce the length of the Fe cathode, thus giving the K x-ray peak from Fe at 6.4 keV. This allows correction of the ^{71}Ge peak position due to the accumulation of polymer de-

posits on the anode wire which may occur after prolonged operation. A $^{109}\text{Cd} + \text{Se}$ source, which gives peaks at 1.4 keV and 11.2 keV, is also occasionally used to check linearity.

The measure of energy is the integral of the pulse waveform for 800 ns after pulse onset. The ^{71}Ge peak position is based on the ^{55}Fe calibration adjusted for polymerization and the energy window (two full widths at half maximum) is set by the ^{55}Fe resolution. If the calibration centroid shifts between two calibrations, the window for energy selection is linearly shifted in time between the two calibrations. Typical gain shifts are of the order of a few percent which leads to a calculated uncertainty in the counting efficiency of no more than -3.1%.

To determine the rise time windows for ^{71}Ge events, proportional counters filled with $^{71}\text{GeH}_4$ are measured in each of the counting channels. All events inside the

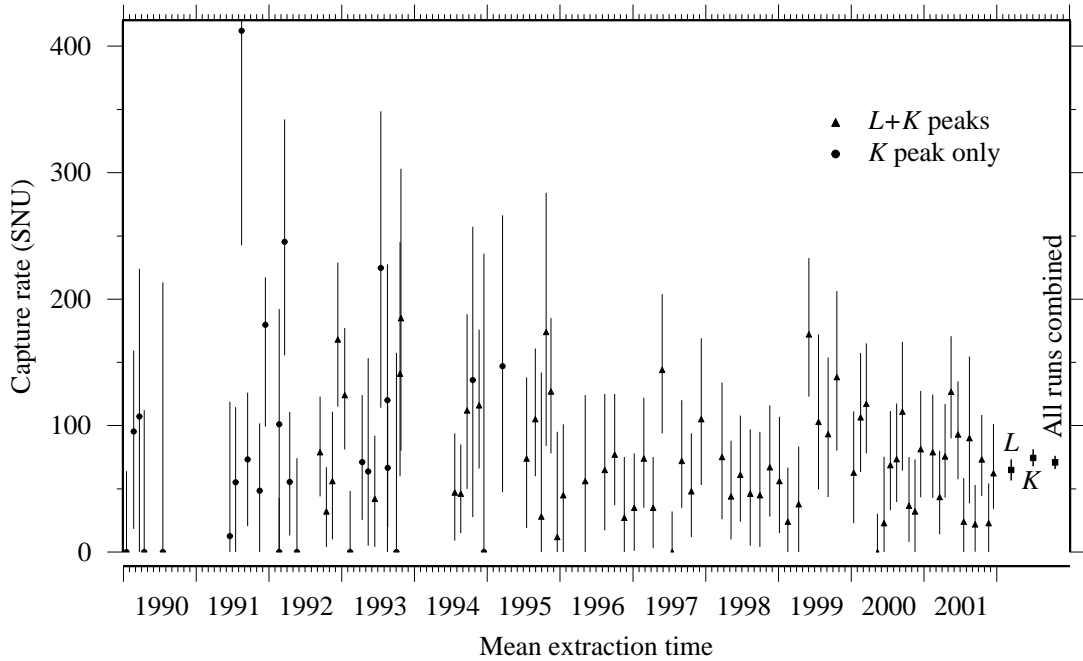


FIG. 1: Capture rate for all SAGE extractions as a function of time. Error bars are statistical with 68% confidence. The combined result of all runs in the L peak, the K peak, and both L and K peaks is shown on the right side. The last 3 runs are still counting and their results are preliminary.

energy windows of the K and L peaks are selected, and the rise time T_N of each event is calculated [18]. The rise time values are arranged in ascending order and limits are set such that 5% of the events are excluded. For a counter filled with 30% GeH_4 this leads to K - and L -peak event selection limits on T_N of 0.0 ns to 18.4 ns and 0.0 ns to 10.0 ns, respectively. The upper limits are reduced to 13.2 ns and 9 ns for the K and L peaks, respectively, when the GeH_4 concentration is in the range of 7% to 15%. The variation with counter filling and electronics channel results in an uncertainty in the efficiency of about $\pm 1\%$. The small loss in counting efficiency associated with this cut leads to a significant reduction in the number of background events.

Table I gives the parameters of the 35 runs from 1998–2001 that are used for solar neutrino measurement.

III. STATISTICAL ANALYSIS OF SOLAR DATA

The selection criteria result in a group of events from each extraction that are candidate ^{71}Ge decays. These events are fit to a maximum likelihood function [19], assuming that they originate from an unknown but constant-rate background and the exponentially decaying rate of ^{71}Ge .

Two time cuts are made on the counting intervals to reduce the effect of radon and radon daughters, which can give pulses that mimic ^{71}Ge . To minimize the effect of Rn that enters the interior of the passive shield when

it is opened for counter calibration, we delete the first 2.6 h of counting time in the K and L peaks after shield openings. Another very dangerous background occurs if even a few atoms of ^{222}Rn enter the counter during filling. Most decays of Rn inside the counter give slow pulses at a saturated energy beyond the ^{71}Ge peaks, but approximately 8% of the pulses from Rn and its daughters make fast pulses that are indistinguishable from those of ^{71}Ge . Since the radon decay chain takes on average 50 min to reach the long-lived isotope ^{210}Pb , deleting 15 min before and 3 h after each saturated pulse removes most of these internal Rn events.

For each individual extraction, the best estimate of the ^{71}Ge production rate is found by maximizing the likelihood function. The statistical uncertainty in the production rate is found by integrating the likelihood function over the background rate to give a function of production rate only, and then finding the minimum range in this rate that includes 68% of the area under the curve. This procedure is done separately for events in the L and K peaks. The small variation in the Earth-Sun distance (no greater than 3%) due to the eccentricity of the Earth's orbit is taken into account. The best estimate for a combination of runs (and also for the $L + K$ combination of a single run) is obtained by multiplying the individual likelihood functions, requiring that the production rate per unit mass of Ga be equivalent but allowing the background rate to be different for each component of the function. The global maximum of the product function is then found and the 68% confidence region for the

TABLE II: Results of combined analysis of K -peak and L -peak events for all runs after 1997. See [20] for the definition and interpretation of Nw^2 . The accuracy of the Monte Carlo-determined goodness of fit probability is $\sim 1.5\%$ for each individual run and $\sim 4\%$ for the combination of all runs. The last 3 runs are still counting and their results are preliminary.

Exposure date	Number of candidate events	Number fit to ^{71}Ge	Best fit (SNU)	68% conf. range (SNU)	Nw^2	Prob. (%)
Apr. 98	39	5.4	75	26–134	0.052	72
May 98	23	3.4	44	10–88	0.051	68
July 98	22	4.8	61	24–108	0.065	52
Aug. 98	33	3.6	46	5–97	0.039	84
Oct. 98	40	3.8	45	4–95	0.028	95
Nov. 98	32	5.9	67	28–116	0.101	30
Jan. 99	21	4.5	56	15–107	0.036	84
Feb. 99	16	1.6	24	0–67	0.114	28
Apr. 99	10	1.8	38	5–83	0.105	36
June 99	14	12.9	172	123–232	0.048	80
July 99	17	5.5	103	49–172	0.118	20
Sep. 99	20	7.1	93	43–154	0.099	28
Oct. 99	16	10.0	138	80–206	0.066	56
Jan. 00	24	5.4	63	23–111	0.060	59
Feb. 00	21	9.1	107	63–157	0.058	55
Mar. 00	19	10.1	117	78–165	0.046	79
May 00	15	0.0	0	0–32	0.143	40
June 00	17	1.4	23	0–75	0.179	17
July 00	29	6.4	69	33–111	0.088	34
Aug. 00	14	5.2	74	39–117	0.086	33
Sep. 00	30	9.2	111	64–166	0.093	24
Oct. 00	14	3.0	37	8–75	0.020	99
Nov. 00	25	2.9	32	0–73	0.208	9
Dec. 00	27	7.6	81	43–127	0.062	68
Feb. 01	21	6.3	79	43–125	0.088	34
Mar. 01	18	3.8	44	14–80	0.120	24
Apr. 01	17	6.7	76	43–117	0.074	45
May 01	21	11.9	127	90–171	0.088	31
June 01	20	9.4	93	57–135	0.025	96
July 01	9	2.0	24	0–58	0.033	92
Aug. 01	21	5.4	90	38–155	0.065	57
Sep. 01	10	2.1	22	0–53	0.139	18
Oct. 01	12	7.5	73	44–109	0.082	41
Nov. 01	15	2.6	23	0–54	0.084	38
Dec. 01	9	5.2	62	34–101	0.063	70
Combined	711	191.8	67	60–74	0.080	42

production rate is set by finding where the function has decreased from its value at the maximum by the factor 0.606, all other variables being maximized. The results of the combined analysis of recent extractions are given in Table II and the results of all runs of SAGE are plotted in Fig. 1.

After publication of Ref. [4], which reported measurements from January 1990 through December 1997, it was found that a faulty data acquisition program was used in the period from June 1996 through December 1999. At the beginning of this period it was necessary to change the hardware that recognized coincidences between the NaI and proportional counters. The new hardware required a modification of the acquisition program which introduced an error in the trigger logic. As a result 23.9 ± 0.4 (stat.) ± 0.5 (syst.)% of triggers was lost. This

error artificially reduced the results of individual runs counting during this period and slightly influenced the overall result. Corrected results were given in [21].

IV. SYSTEMATIC EFFECTS

Table III summarizes the systematic effects that may affect the measured solar neutrino capture rate. These uncertainties fall into three main categories: those associated with extraction efficiency, with counting efficiency, and with backgrounds. Some of these effects were mentioned above and the others will be briefly discussed here.

The counting efficiency and its uncertainty was determined by a series of measurements with gas fillings of ^{71}Ge , ^{37}Ar , and ^{69}Ge . The uncertainty contains terms

TABLE III: Summary of systematic effects and their uncertainties in SNU. The values for extraction and counting efficiencies are based on a rate of 70.8 SNU.

Extraction efficiency	Ge carrier mass	± 1.5
	Extracted Ge mass	± 1.8
	Residual carrier Ge	± 0.6
	Ga mass	± 0.2
Counting efficiency	Counter effects	± 1.3
	Gain shifts	$+2.2$
	Resolution	$-0.4, +0.5$
	Rise time limits	± 0.7
	Lead and exposure times	± 0.6
Backgrounds	Neutrons	<-0.02
	U and Th	<-0.7
	muons	<-0.7
	Internal radon	<-0.2
	External radon	0.0
	Other Ge isotopes	<-0.7
Total		$-3.2, +3.7$

due to volume efficiency, end effects, and gas efficiency. Adding each of these effects in quadrature gives a $\pm 1.8\%$ uncertainty due to the counters.

There exist small contributions to the ^{71}Ge signal by means other than solar neutrinos. Limits on the creation of ^{71}Ge through the (n, p) reaction on ^{71}Ga and by cosmic-ray muons were obtained by measurement in the Ga chamber of both the fast neutron [16, 22] and muon fluxes [15]. Limiting values on the U and Th concentration in the Ga, which can also make ^{71}Ge , have been determined by low background counting in a Ge detector [23] and by glow discharge mass spectrometry [24]. The inferred ^{71}Ge production rate from the combination of all of these processes is no more than 1 SNU.

Rn decay in the vicinity of the proportional counters or inside the counters themselves can also give events that mimic ^{71}Ge decay. To reduce such events Rn is purged from the volume near the counters by a constant flow of gas from boiling liquid nitrogen and special anti-Rn procedures are applied to purify the gas mixture at the time of counter filling. The influence of residual Rn was quantified by studies in which Rn was added inside the counter [25] and the response of the counter to external gamma-rays was measured [26]. The systematic uncertainties on the ^{71}Ge production rate for Rn that remains after the time cuts were determined to be <0.2 SNU for internal Rn and 0.03 SNU for external Rn.

^{68}Ge and ^{69}Ge can be produced by background processes and their decays can be misinterpreted as ^{71}Ge . ^{68}Ge is of special concern as it decays solely by electron capture giving events that are identical to those from ^{71}Ge . It is mainly produced by cosmic-ray muons and we can estimate the rate by scaling the predicted ^{71}Ge rate of 0.012 ± 0.06 atoms/day in 60 t of Ga [4, 27] by the measured cross section ratio for ^{68}Ge to ^{71}Ge pro-

duction with 280-GeV muons of 2.2 ± 0.1 [28]. This gives 0.022 ± 0.013 atoms of ^{68}Ge produced by muons per day in 50 t of Ga. Since the ^{68}Ge half life is 271 d, considerably longer than the usual total counting time, these pulses will be distributed almost uniformly during the counting period, but there will be a small excess during the early part of counting. Using typical values for exposure time of 30 d, Ga mass of 50 t, extraction efficiency of 0.9, counting efficiency of 0.6 in the sum of L and K peaks, 150 d of counting, and our average $L + K$ background rate of 0.175/day, simulations show that a true ^{68}Ge production rate of 0.022/day leads to a false ^{71}Ge production rate of 0.0085/day, which is equivalent to 0.05 SNU.

The isotope ^{69}Ge can be produced from Ga by several processes, including the interaction of cosmic rays, ^8B solar neutrinos, and protons on ^{71}Ga , where the protons are secondaries either from α particles from internal radioactivity or from neutrons from the surrounding rock. The total ^{69}Ge production rate in 60 t of Ga is estimated to be 0.21 atoms/day [4] with an uncertainty of approximately 50%. Because most ^{69}Ge decays are accompanied by gamma rays which are rejected by the NaI veto with an efficiency of 90%, and counting usually begins ~ 1.5 d after extraction, a time comparable with the ^{69}Ge half life of 1.6 d, we calculate that only 0.045 ^{69}Ge decays will be observed in a typical run [4], a factor of 100 less than the average number of detected ^{71}Ge decays. The background effect of ^{69}Ge is thus no more than 0.7 SNU.

These estimates of the counting rate of ^{68}Ge and ^{69}Ge can be checked by searching for these isotopes in the large set of ^{71}Ge counting data that we now have from solar runs. The procedures and efficiencies for selecting candidate events are described in Ref. [29]. The ^{68}Ge production rate determined in this way is $0.18^{+0.13}_{-0.12}$ atoms/day in 60 t of Ga. The central value is a factor of 7 more than the estimate given above, but within the large error range the rates determined by the two methods are in agreement. Since the result from the cosmic-ray production rate of ^{71}Ge and the cross section ratio has the smaller uncertainty, we use it for our estimate of the ^{68}Ge background. There is some concern though that the predicted cosmic-ray production rate of ^{71}Ge may be underestimated; a more direct measurement would be desirable and this is considered briefly in [29]. A similar search for ^{69}Ge events shows that the production rate in 60 t of gallium is less than 0.49 atoms/day, in agreement with the value given above.

V. RESULTS

The global best fit capture rate for all data from January 1990 to December 2001 (92 runs and 158 separate counting sets) is $70.8^{+5.3}_{-5.2}$ SNU, where the uncertainty is statistical only. In the windows that define the L and K peaks there are 1723 counts with 406.4 assigned by time analysis to ^{71}Ge (the total counting live

time is 29.5 years). If one considers the L -peak and K -peak data independently, the results are $64.8^{+8.5}_{-8.2}$ SNU and $74.4^{+6.8}_{-6.6}$ SNU, respectively. The agreement between the two peaks serves as a strong check on the robustness of the event selection criteria. The total systematic uncertainty is determined by adding in quadrature all the contributions given in Table III. Our overall result is thus $70.8^{+5.3+3.7}_{-5.2-3.2}$ SNU. For comparison, the latest result of the GNO experiment (including GALLEX) is $74.1^{+5.4+4.0}_{-5.4-4.2}$ SNU [13]. If we combine the SAGE statistical and systematic uncertainties in quadrature, the result is $70.8^{+6.5}_{-6.1}$ SNU.

A. Tests of ^{71}Ge Extraction Efficiency

The validity of this result relies on the ability to chemically remove with a well known efficiency a few atoms of ^{71}Ge produced by neutrino interactions from 5×10^{29} atoms of Ga. To measure this efficiency about 350 μg of stable Ge carrier is added to the Ga at the beginning of each exposure, but even after this addition, the separation factor of Ge from Ga is still 1 atom in 10^{11} . We have performed several auxiliary measurements which confirmed that the technology of our experiment has the capability to extract ^{71}Ge at this level.

An initial test was carried out in which Ge carrier doped with a known number of ^{71}Ge atoms was added to a reactor holding 7 t of Ga. Three successive extractions were made, and the number of ^{71}Ge atoms in each extraction was determined by counting. The results [17] showed that the extraction efficiency for the natural Ge carrier and the ^{71}Ge atoms did not differ.

A second experiment addressed the concern that the ^{71}Ge atom from inverse beta decay may be created in an excited or ionized state which results in the ^{71}Ge being tied up in a chemical form from which we cannot efficiently extract. A set of measurements designed to test directly this question was carried out by observing the beta decay of radioactive Ga isotopes in liquid Ga. These measurements [17] showed that the expected isotopes are formed in the amounts anticipated at the 10% level.

A test of all the experimental procedures including the chemical extraction, counting, and the analysis technique was performed using a 19.1 PBq (517 kCi) ^{51}Cr neutrino source. The result, expressed as the ratio of the measured ^{71}Ge production rate to that expected due to the source strength, is 0.95 ± 0.12 [30, 31]. This value provides strong verification that the experimental efficiencies are as claimed and validates the fundamental assumption in radiochemical experiments that the extraction efficiency of atoms produced by neutrino interactions is the same as that of the natural carrier.

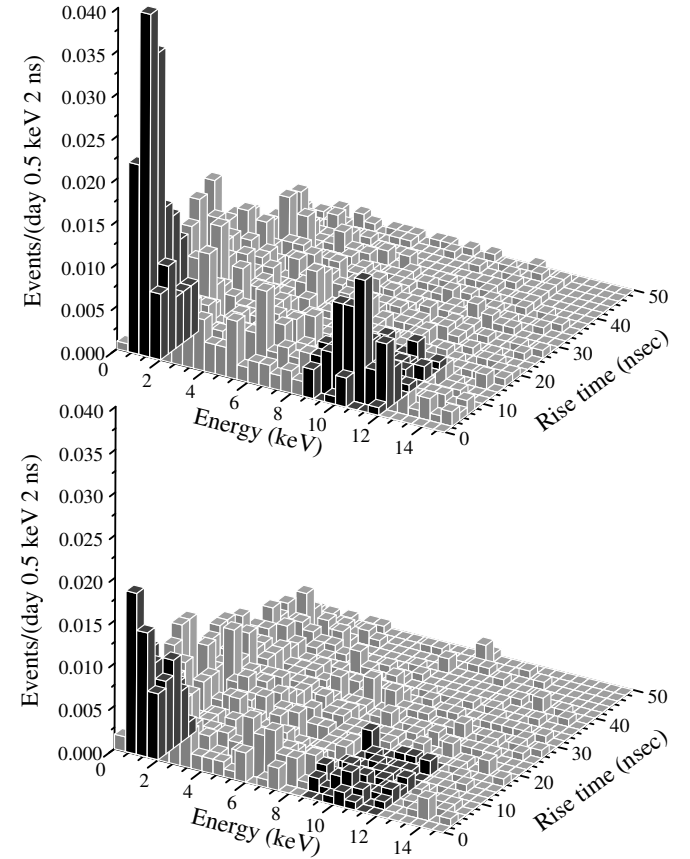


FIG. 2: Upper panel shows a histogram of energy vs rise time for all events observed during the first 22.86 days after extraction for all runs that could be counted in both L and K peaks (except May 1996). The live time is 1169.9 days. The approximate expected location of the ^{71}Ge L and K peaks as predicted by calibrations is shown darkened. Lower panel shows the same histogram for all events that occurred during an equal live time interval beginning at day 100 after the time of extraction.

B. Tests of Analysis Hypotheses

Direct visual evidence that we are really observing ^{71}Ge is in Fig. 2 which shows all events that survive the time cuts and that do not have a NaI coincidence. The expected location of the ^{71}Ge L and K peaks is shown darkened. These peaks are apparent in the upper panel but missing in the lower panel because the ^{71}Ge has decayed away.

1. Time sequence

A major analysis hypothesis is that the time sequence of observed events for each run consists of the superposition of events from the decay of a fixed number of ^{71}Ge atoms plus background events which occur at a constant rate. The quantity Nw^2 and the goodness of fit proba-

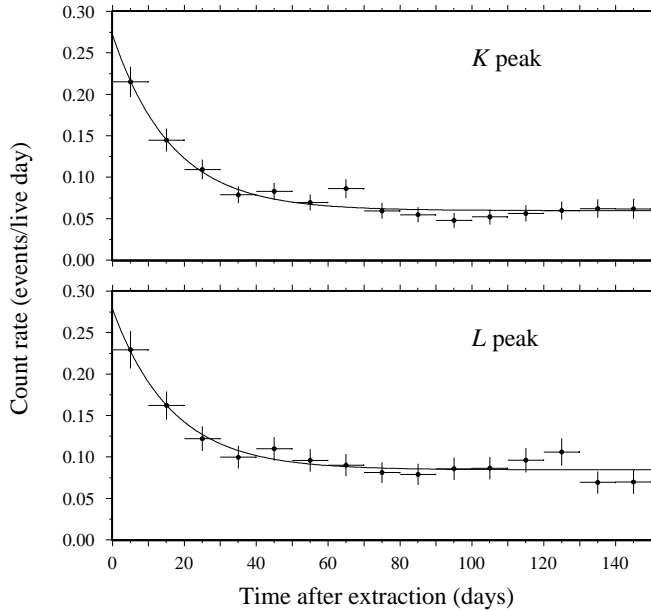


FIG. 3: Count rate for all runs from January 1990 in L and K peaks. The solid line is a fit to the data points with the 11.4-day half-life of ${}^{71}\text{Ge}$ plus a constant background. The vertical error bar on each point is proportional to the square root of the number of counts and is shown only to give the scale of the error. The horizontal error bar is ± 5 d, equal to the 10-day bin size.

bility inferred from it provide a quantitative measure of how well the data fit this hypothesis. These numbers are evaluated for each data set and given in Table II. There are occasional runs with low probability of occurrence, but no more of these are observed than are expected due to normal statistical variation.

This method can also be used to determine the goodness of fit for the combined time sequence of all L plus K events from any combination of runs. For all SAGE runs this test yields $Nw^2 = 0.053$, with a goodness of fit probability of $(72.0 \pm 4.5)\%$. A visual indication of the good quality of this fit is provided in Fig. 3 which shows the count rate for all events in the L and K peaks vs time after extraction. An additional quantitative indication that ${}^{71}\text{Ge}$ is being counted can be obtained by allowing the decay constant during counting to be a free variable in the maximum likelihood fit, along with the combined ${}^{71}\text{Ge}$ production rate and all the background rates. The best fit half-life to all selected events in both L and K peaks is then $9.7^{+1.5}_{-1.3}$ days, in agreement with the measured value [32] of 11.43 days.

2. Production rate sequence

Another analysis hypothesis is that the rate of ${}^{71}\text{Ge}$ production is constant in time. By examination of Fig. 1, it is apparent that, within the large statistical uncer-

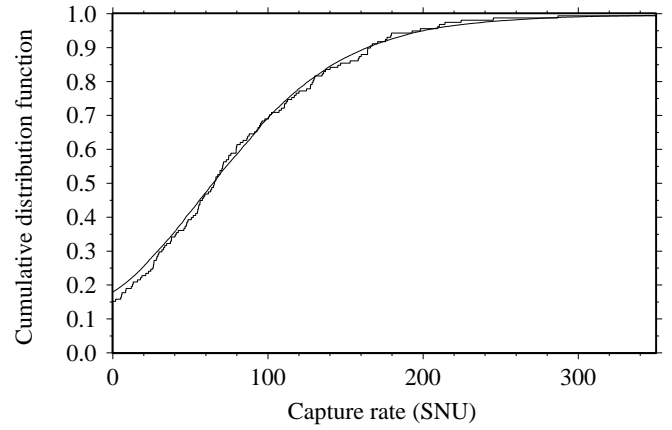


FIG. 4: Cumulative distribution function of the measured neutrino capture rate for all 158 SAGE data sets (jagged curve) and the expected distribution derived by 1000 Monte Carlo simulations of each set (smooth curve). The capture rate in the simulations was assumed to be 70.8 SNU.

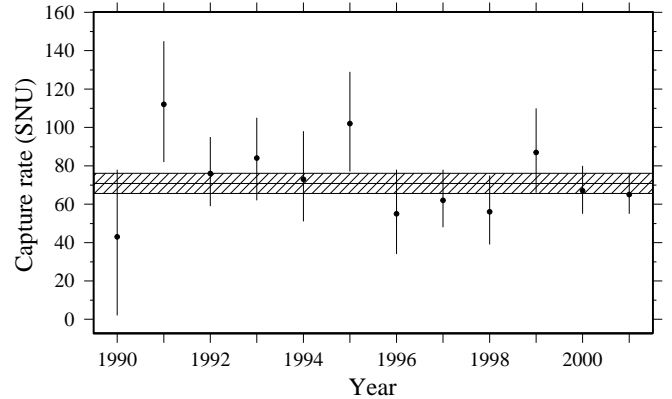


FIG. 5: Combined SAGE results for each year. Shaded band is the combined best fit and its uncertainty for all years. Error bars are statistical with 68% confidence.

tainty for each run, there is no substantial long-term deviation from constancy.

Another way to consider this question is to use the cumulative distribution function of the production rate $C(p)$, defined as the fraction of data sets whose production rate is less than p . Figure 4 shows this distribution for all data sets and the expected distribution from simulation, assuming a constant production rate of 70.8 SNU. The two curves parallel each other closely and can be compared by calculating the Nw^2 test statistic [20]. This gives $Nw^2 = 0.337$ whose probability is 11%.

C. Temporal Combinations of Data

If vacuum oscillations were the reason why the capture rate in Ga is reduced compared with the predicted rate

TABLE IV: Results of combined analysis of all runs during yearly, monthly, and bimonthly intervals. Runs are assigned to each time period by their mean exposure time. The accuracy of the probability estimate is $\sim 4\%$.

Exposure interval	Number of data sets	Number of candidate events	Number fit to ^{71}Ge	Best fit (SNU)	68% conf. range (SNU)	Nw^2	Probability (%)
1990	5	43	4.9	43	2– 78	0.260	9
1991	6	59	25.5	112	82– 145	0.120	17
1992	13	145	39.8	76	59– 95	0.047	68
1993	15	97	33.2	84	62– 105	0.199	6
1994	10	155	24.1	73	51– 98	0.027	95
1995	13	210	37.7	102	77– 129	0.041	82
1996	10	120	19.3	55	34– 78	0.067	51
1997	16	183	35.7	62	48– 78	0.057	62
1998	12	189	26.7	56	39– 75	0.064	60
1999	14	114	40.8	87	66– 110	0.068	33
2000	22	235	62.2	67	55– 80	0.102	29
2001	22	173	64.4	65	55– 76	0.050	70
January	11	129	24.8	58	37– 80	0.082	35
February	12	101	25.5	60	44– 77	0.045	74
March	9	129	34.5	102	79– 127	0.043	78
April	9	80	16.9	54	37– 73	0.072	39
May	12	114	34.7	75	59– 94	0.051	62
June	11	101	33.6	79	58– 102	0.175	5
July	15	176	26.6	52	37– 69	0.091	35
August	15	161	38.7	78	60– 96	0.058	51
September	20	220	48.4	68	54– 84	0.035	91
October	17	169	40.3	73	57– 91	0.080	45
November	15	196	37.5	59	44– 75	0.034	82
December	12	147	46.4	105	84– 127	0.040	89
January+February	23	230	50.5	59	46– 73	0.095	34
March+April	18	209	49.2	75	61– 91	0.026	> 99
May+June	23	215	68.0	77	63– 91	0.111	10
July+August	30	337	65.4	65	53– 78	0.075	50
September+October	37	389	88.7	70	59– 82	0.041	85
November+December	27	343	84.3	78	66– 91	0.042	85
February+March	21	230	58.8	77	63– 91	0.037	84
April+May	21	194	50.8	66	54– 79	0.049	60
June+July	26	277	58.7	63	50– 77	0.081	42
August+September	35	381	87.1	72	61– 84	0.043	84
October+November	32	365	78.0	66	54– 78	0.043	84
December+January	23	276	73.6	84	70– 99	0.059	65
February+November	27	297	63.1	59	48– 71	0.017	99
March+October	26	298	75.1	84	71– 99	0.062	66
April+September	29	300	64.2	63	52– 75	0.043	86
May+August	27	275	73.3	77	64– 89	0.045	75

of the standard solar model, then a seasonal variation of the rate is expected for some values of the parameters [33, 34]. Other phenomena can also yield temporal variations (see, e.g., [35, 36]). We thus give in Table IV the results of combining the SAGE runs in various ways, monthly, bimonthly and yearly. There is no compelling evidence for a temporal variation in any of these data divisions. The yearly results are plotted in Fig. 5 which shows that the rate has been more or less constant during the data taking period. Considering only the statistical errors, a χ^2 test against the hypothesis of the constant rate of 70.8 SNU yields $\chi^2 = 6.6$, which, with 11 degrees of freedom, has a probability of 83%.

VI. THE pp NEUTRINO FLUX

One of the main purposes of the Ga experiment is to provide information that leads to the experimental determination of the flux of pp neutrinos at the Earth. In this Section we indicate the present state of this measurement where we use only information from the various solar neutrino experiments and assume that their reduced capture rate compared to SSM predictions is due to neutrino oscillations.²

² Note that the very restrictive luminosity constraint [38] is not used here.

By combining the results of SAGE, GALLEX, and GNO, the capture rate in the Ga experiment is approximately 72 ± 5 SNU. This rate is the sum of the rates from all the components of the solar neutrino flux, which we denote by $[pp + {}^7\text{Be} + \text{CNO} + pep + {}^8\text{B}|\text{Ga,exp}]$, where “exp” indicates that this is a measured rate. (We ignore the *hep* contribution, as it is a negligible 0.05% of the total in the SSM calculation [9].)

The only one of these flux components that is known is the ${}^8\text{B}$ flux, measured by SNO to be $[{}^8\text{B}|\text{SNO,exp}] = (1.75 \pm 0.15) \times 10^6$ electron neutrinos/(cm²-s) [2]. Since the shape of the ${}^8\text{B}$ spectrum in SNO and SuperKamiokande is very close to that of the SSM above 5 MeV and the cross section for Ga rises steeply with energy, we can use the SNO flux and the cross section for ${}^8\text{B}$ neutrinos with SSM shape $(2.40^{+0.77}_{-0.36} \times 10^{-42}$ cm²) to conclude that the ${}^8\text{B}$ contribution to the Ga experiment is $[{}^8\text{B}|\text{Ga,exp}] = 4.2^{+1.4}_{-0.7}$ SNU. Subtracting this measured value from the total Ga rate gives $[pp + {}^7\text{Be} + \text{CNO} + pep|\text{Ga,exp}] = 67.8^{+5.1}_{-5.2}$ SNU.

The measured capture rate in the Cl experiment is $[{}^7\text{Be} + {}^8\text{B} + \text{CNO} + pep|\text{Cl,exp}] = 2.56 \pm 0.23$ SNU [3]. (The *hep* contribution will again be neglected as it is only 0.5% of the total in the SSM.) Since the cross section in Cl is dominated by neutrinos above 5 MeV, we can again use the SNO flux and the cross section calculated for the SSM ($1.14^{+0.04}_{-0.04} \times 10^{-42}$ cm²), and deduce that the contribution of ${}^8\text{B}$ to the Cl experiment is $[{}^8\text{B}|\text{Cl,exp}] = 2.00 \pm 0.18$ SNU. Subtracting this component from the total leaves $[{}^7\text{Be} + \text{CNO} + pep|\text{Cl,exp}] = 0.56 \pm 0.29$ SNU, all of which is due to neutrinos of medium energy.

Neutrino oscillations have the effect of introducing an energy-dependent survival factor to the fluxes predicted by the SSM. For the medium-energy neutrinos this factor for the Cl experiment can be approximated by the ratio of the measured rate to the SSM prediction of $[{}^7\text{Be} + \text{CNO} + pep|\text{Cl,SSM}] = 1.79 \pm 0.23$ SNU. If we assume that the survival factor varies slowly with energy, we find it to be given by $[{}^7\text{Be} + \text{CNO} + pep|\text{Cl,exp}] / [{}^7\text{Be} + \text{CNO} + pep|\text{Cl,SSM}] = 0.31 \pm 0.17$. Since the ${}^7\text{Be}$ contribution dominates, and it is at a single energy, the error in this factor due to the assumption that it is the same for all of these flux components can be estimated by considering the contribution of the non- ${}^7\text{Be}$ components to the total in the SSM, which is 36%. We thus increase the error from 0.17 to $0.17 + 0.31 \times 0.36 = 0.28$.

The relative contributions to the capture rate of the medium-energy neutrinos are about the same in Ga as in Cl (75% from ${}^7\text{Be}$ in Ga compared to 64% in Cl). Thus it is reasonable to apply the survival factor determined for Cl to the Ga experiment, i.e., $[{}^7\text{Be} + \text{CNO} + pep|\text{Ga,exp}] = (0.31 \pm 0.28) \times [{}^7\text{Be} + \text{CNO} + pep|\text{Ga,SSM}] = 14.4 \pm 13.0$ SNU. We subtract this contribution from the rate above and get the result for the measured *pp* rate in the Ga experiment $[pp|\text{Ga,exp}] = [pp + {}^7\text{Be} + \text{CNO} + pep|\text{Ga,exp}] - [{}^7\text{Be} + \text{CNO} + pep|\text{Ga,exp}] = 53 \pm 14$ SNU.

Since the cross section does not change appreciably

over the narrow range of Ga response to the *pp* neutrinos, (0.23–0.42) MeV, we divide the capture rate by the SSM cross section for electron neutrinos of $11.7^{+0.3}_{-0.3} \times 10^{-46}$ cm² and obtain the measured electron neutrino *pp* flux at Earth of $(4.6 \pm 1.2) \times 10^{10}$ /(cm²-s). Alternatively, if we divide the capture rate by the cross section multiplied by the survival probability for *pp* neutrinos, which is 60% for the favored LMA solution [9] assuming no transitions to sterile neutrino flavors, we receive the rate of *pp* neutrino emission in the solar fusion reaction of $(7.6 \pm 2.0) \times 10^{10}$ /(cm²-s), in agreement with the SSM calculation of $(5.95 \pm 0.06) \times 10^{10}$ /(cm²-s) [37]. The major component of the error in the *pp* flux measurement is due to the poor knowledge of the energy-dependent survival factor.

Several approximations were made in arriving at this value, whose nature cannot be easily quantified, so perhaps the error given here is somewhat underestimated. Nonetheless, as mentioned in the Introduction, it will be possible to reduce the error in this flux greatly when the region of mass and mixing angle parameters is better determined, as should be done by the KamLAND experiment, and when the ${}^7\text{Be}$ flux is directly measured, as anticipated by Borexino. The dominant error should eventually be due to the inaccuracy of the Ga measurement itself, and hence we are seeking to reduce our statistical and systematic errors.

VII. SUMMARY AND CONCLUSIONS

The methods and analysis of the SAGE experiment have been summarized and results for 92 extractions during 12 years of operation from January 1990 through December 2001 have been presented. The measured capture rate is $70.8^{+5.3}_{-5.2}$ SNU where the uncertainty is statistical only. Analysis of all known systematic effects indicates that the total systematic uncertainty is $^{+3.7}_{-3.2}$ SNU, less than the statistical error. Finally we have examined the counting data and shown that there is good evidence that ${}^{71}\text{Ge}$ is being counted, that the counting data fit the analysis hypotheses, and that the counting data are self-consistent.

The SAGE result of 70.8 SNU represents 54% of SSM predictions [9]. Given the extensive systematic checks and auxiliary measurements that have been performed, especially the ${}^{51}\text{Cr}$ neutrino source experiment [30, 31], this 6.2σ reduction of the solar neutrino capture rate compared to SSM predictions is very strong evidence that the solar neutrino spectrum below 2 MeV is significantly depleted, as has been proven for the ${}^8\text{B}$ flux by the Cl, Kamiokande, and SNO experiments. The SAGE result is even somewhat below the astrophysical minimum capture rate of $79.5^{+2.3}_{-2.0}$ SNU [39].

Several recent phenomonology papers (see, e.g., [40, 41, 42]) discuss the combined fit of all solar neutrino experiments. Their conclusion is that the electron neutrino oscillates into other species and the best fit is to the LMA

region of Mikheyev-Smirnov-Wolfenstein (MSW) oscillations. To more precisely determine the oscillation parameters in the solar sector will require additional data, especially from experiments sensitive to the low-energy neutrinos. In this vein, SAGE continues to perform regular solar neutrino extractions every four weeks with ~ 50 t of Ga and will continue to reduce its statistical and systematic uncertainties.

Acknowledgments

We thank J. N. Bahcall, M. Baldo-Ceolin, G. T. Garvey, W. Haxton, V. A. Kuzmin, V. V. Kuzminov, V. A. Matveev, L. B. Okun, R. G. H. Robertson, V. A. Rubakov, A. Yu. Smirnov, A. N. Tavkhelidze, and many members of GALLEX and GNO for their continued interest and for stimulating discussions. We

greatly appreciate the work of our prior collaborators O. L. Anosov, O. V. Bychuk, M. L. Cherry, R. Davis, Jr., I. I. Knyshenko, V. N. Kornoukhov, R. T. Kouzes, K. Lande, A. V. Ostrinsky, D. L. Wark, P. W. Wildenhain, and Yu. I. Zakharov. We acknowledge the support of the Russian Academy of Sciences, the Institute for Nuclear Research of the Russian Academy of Sciences, the Russian Ministry of Science and Technology, the Russian Foundation of Fundamental Research under grant No. 96-02-18399, the Division of Nuclear Physics of the U.S. Department of Energy under grant No. DEFG03-97ER41020, and the U.S. Civilian Research and Development Foundation under award No. RP2-159. This research was made possible in part by grant No. M7F000 from the International Science Foundation and grant No. M7F300 from the International Science Foundation and the Russian Government.

[1] S. Fukuda *et al.*, hep-ex/0103032, Phys. Rev. Lett. **86**, 5651 (2001); hep-ex/0103033, Phys. Rev. Lett. **86**, 5656 (2001).

[2] Q. R. Ahmad *et al.*, nucl-ph/0106015, Phys. Rev. Lett. **87**, 071301 (2001).

[3] B. T. Cleveland, T. J. Daily, R. Davis, Jr., J. R. Distel, K. Lande, C. K. Lee, and P. S. Wildenhain, Astrophys. J. **496**, 505 (1998).

[4] J. N. Abdurashitov, V. N. Gavrin, S. V. Girin, V. V. Gorbatchev, T. V. Ibragimova, A. V. Kalikhov, N. G. Khairnasov, T. V. Knodel, I. N. Mirmov, A. A. Shikhin, E. P. Veretenkin, V. M. Vermul, V. E. Yants, G. T. Zatsepina, T. J. Bowles, W. A. Teasdale, D. L. Wark, M. L. Cherry, J. S. Nico, B. T. Cleveland, R. Davis, Jr., K. Lande, and P. S. Wildenhain, S. R. Elliott and J. F. Wilkerson, astro-ph/9907113, Phys. Rev. C **60**, 055801 (1999).

[5] W. Hampel, J. Handt, G. Heusser, J. Kiko, T. Kirsten, M. Laubenstein, E. Pernicka, W. Rau, M. Wojcik, Y. Zakharov, R. v. Ammon, K. H. Ebert, T. Fritsch, E. Henrich, L. Stielglitz, F. Weirich, M. Balata, M. Sann, F. X. Hartmann, E. Bellotti, C. Cattadori, O. Cremonesi, N. Ferrari, E. Fiorini, L. Zanotti, M. Altmann, F. v. Feilitzsch, R. Mößbauer, S. Wänninger, G. Berthomieu, E. Schatzmann, I. Carmi, I. Dostrovsky, C. Bacci, P. Belli, R. Bernabei, S. d'Angelo, L. Paoluzi, M. Cribier, J. Rich, M. Spiro, C. Tao, D. Vignaud, J. Boger, R. L. Hahn, J. K. Rowley, R. W. Stoenner, and J. Wenner, Phys. Lett. B **447**, 127 (1999).

[6] Y. Fukuda *et al.*, Phys. Rev. Lett. **77**, 1683 (1996).

[7] See www.sns.ias.edu/~jnb/Meetings/Lownu/index.html and www-sk.icrr.u-tokyo.ac.jp/lownu/index.html.

[8] V. A. Kuzmin, Zh. Eksp. Teor. Fiz. **49**, 1532 (1965) (Sov. Phys. JETP **22**, 1051 (1966)).

[9] J. N. Bahcall, M. C. Gonzalez-Garcia, and C. Peña-Garay, hep-ph/0111150.

[10] A. S. Brun, S. Turck-Chièze, and P. Morel, astro-ph/9806272, Astrophys. J. **506**, 913 (1998).

[11] A. Piepke, Nucl. Phys. B (Proc. Suppl.) **91**, 99 (2001).

[12] G. Alimonti *et al.*, (BOREXINO collaboration), *Science and Technology of BOREXINO: a real-time detector for low-energy solar neutrinos*, hep-ex/0012030, Astroparticle Physics (subm.).

[13] M. Altmann, M. Balata, P. Belli, E. Bellotti, R. Bernabei, E. Burkert, C. Cattadori, G. Cerichelli, M. Chiarini, M. Cribier, S. d'Angelo, G. Del Re, K. H. Ebert, F. v. Feilitzsch, N. Ferrari, W. Hampel, J. Handt, E. Henrich, G. Heusser, J. Kiko, T. Kirsten, T. Lachenmaier, J. Lanfranchi, M. Laubenstein, D. Motta, W. Rau, H. Richter, S. Wänninger, M. Wojcik, L. Zanotti, hep-ex/0006034, Phys. Lett. **490**, 16 (2000).

[14] V. N. Gavrin, V. N. Kornoukhov, and G. T. Zatsepina, Institute for Nuclear Research of the Academy of Sciences of the USSR Report No. P-0690, 1991.

[15] V. N. Gavrin, V. E. Gurentsov, V. N. Kornoukhov, A. M. Pshukov, and A. A. Shikhin, Institute for Nuclear Research of the Academy of Sciences of the USSR Report No. P-0698, 1991.

[16] J. N. Abdurashitov, V. N. Gavrin, A. V. Kalikhov, V. L. Matushko, A. A. Shikhin, V. E. Yants, and O. S. Zaborskaya, to be published in Proceedings of the XIth Int. School on Particles and Cosmology, Baksan, Russia, April 2001.

[17] J. N. Abdurashitov, E. L. Faizov, V. N. Gavrin, A. O. Gusev, A. V. Kalikhov, T. V. Knodel, I. I. Knyshenko, V. N. Kornoukhov, I. N. Mirmov, A. M. Psukhov, A. M. Shalagin, A. A. Shikhin, P. V. Timofeyev, E. P. Veretenkin, V. M. Vermul, G. T. Zatsepina, T. J. Bowles, S. R. Elliott, J. S. Nico, W. A. Teasdale, D. L. Wark, J. F. Wilkerson, B. T. Cleveland, T. Daily, R. Davis, K. Lande, C. K. Lee, P. S. Wildenhain, M. L. Cherry, and R. T. Kouzes, Phys. Lett. B **328**, 234 (1994).

[18] S. R. Elliott, Nucl. Instrum. Methods Phys. Res. A **290**, 158 (1990).

[19] B. T. Cleveland, Nucl. Instrum. Methods Phys. Res. **214**, 451 (1983).

[20] B. T. Cleveland, Nucl. Instrum. Methods Phys. Res. A **416**, 405 (1998).

[21] V. N. Gavrin, Proceedings of the XIXth International

Conf. on Neutrino Physics and Astrophysics, Sudbury, Canada, 16–21 June 2000, ed. by J. Law, R. W. Ollerhead, and J. J. Simpson, Nucl. Phys. B (Proc. Suppl.) **91**, 36 (2000).

[22] V. N. Gavrin, V. N. Kornoukhov, and V. E. Yants, Institute for Nuclear Research of the Academy of Sciences of the USSR Report No. P-0703, 1991.

[23] V. N. Gavrin, S. N. Danshin, A. V. Kopylov, and V. E. Cherekhovsky, Institute for Nuclear Research of the Academy of Sciences of the USSR Report No. P-0494, 1986.

[24] Charles Evans Associates report (unpublished).

[25] V. N. Gavrin, V. V. Gorbachev, and I. N. Mirmov, *Yad. Phys.* (subm.).

[26] V. N. Gavrin and V. V. Gorbachev, *Yad. Phys.* (subm.).

[27] V. N. Gavrin and Yu. I. Zacharov, Institute for Nuclear Research of the Academy of Sciences of the USSR Report No. P-0560, 1987.

[28] M. Cribier, B. Pichard, J. Rich, J. P. Soirat, M. Spiro, Th. Stolarczyk, C. Tao, D. Vignaud, P. Anselmann, A. Lenzing, C. Schlosser, R. Wink, and J. K. Rowley, *Astropart. Phys.* **6**, 129 (1997).

[29] V. N. Gavrin, V. V. Gorbachev, T. V. Ibragimova, and B. T. Cleveland, *Yad. Phys.* (subm.).

[30] J. N. Abdurashitov, V. N. Gavrin, S. V. Girin, V. V. Gorbachev, T. V. Ibragimova, A. V. Kalikhov, N. G. Khairnasov, T. V. Knodel, V. N. Kornoukhov, I. N. Mirmov, A. A. Shikhin, E. P. Veretenkin, V. M. Vermul, V. E. Yants, G. T. Zatsepin, T. J. Bowles, J. S. Nico, W. A. Teasdale, D. L. Wark, M. L. Cherry, V. N. Karaulov, V. L. Levitin, V. I. Maev, P. I. Nazarenko, V. S. Shkol'nik, N. V. Skorikov, B. T. Cleveland, T. Daily, R. Davis, Jr., K. Lande, C. K. Lee, P. S. Wildenhain, Yu. S. Khomyakov, A. V. Zvonarev, S. R. Elliott, and J. F. Wilkerson, *Phys. Rev. Lett.* **77**, 4708 (1996).

[31] J. N. Abdurashitov, V. N. Gavrin, S. V. Girin, V. V. Gorbachev, T. V. Ibragimova, A. V. Kalikhov, N. G. Khairnasov, T. V. Knodel, V. N. Kornoukhov, I. N. Mirmov, A. A. Shikhin, E. P. Veretenkin, V. M. Vermul, V. E. Yants, G. T. Zatsepin, Yu. S. Khomyakov, A. V. Zvonarev, T. J. Bowles, J. S. Nico, W. A. Teasdale, D. L. Wark, M. L. Cherry, V. N. Karaulov, V. L. Levitin, V. I. Maev, P. I. Nazarenko, V. S. Shkol'nik, N. V. Skorikov, B. T. Cleveland, T. Daily, R. Davis, Jr., K. Lande, C. K. Lee, P. S. Wildenhain, S. R. Elliott, and J. F. Wilkerson, hep-ph/9803418, *Phys. Rev. C* **59**, 2246 (1999).

[32] W. Hampel and L. Remsberg, *Phys. Rev. C* **31**, 666 (1985).

[33] V. Berezinsky, G. Fiorentini, and M. Lissia, hep-ph/9904225, *Astropart. Phys.* **12**, 299 (2000).

[34] G. L. Fogli, E. Lisi, D. Montanino, and A. Palazzo, hep-ph/9910387, *Phys. Rev. D* **61**, 073009 (2000).

[35] J. Pulido and E. Kh. Akhmedov, hep-ph/9907399, *Astropart. Phys.* **13**, 227 (2000).

[36] P. A. Sturrock and J. D. Scargle, astro-ph/0011228, *Astrophys. J.* **550**, L101-L104 (2001).

[37] J. N. Bahcall, M. H. Pinsonneault, and S. Basu, astro-ph/0010346, *Astrophys. J.* **555**, 990-1012 (2001).

[38] J. N. Bahcall, hep-ph/0108148, *Phys. Rev. C* **65** 025801 (2002).

[39] J. N. Bahcall, hep-ph/9710491, *Phys. Rev. C* **56**, 3391 (1997).

[40] J. N. Bahcall, M. C. Gonzalez-Garcia, and C. Peña-Garay, hep-ph/0106258, *JHEP* **0108**, 014 (2001).

[41] P. I. Krastev and A. Yu. Smirnov, hep-ph/0108177.

[42] M. C. Gonzalez-Garcia, M. Maltoni, and C. Peña-Garay, hep-ph/0108073.